

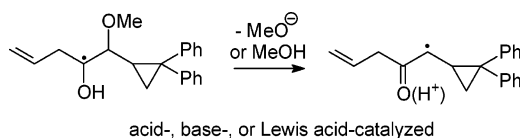
Acid-, Base-, and Lewis-Acid-Catalyzed Heterolysis of Methoxide from an α -Hydroxy- β -methoxy Radical: Models for Reactions Catalyzed by Coenzyme B₁₂-Dependent Diol Dehydratase

Libin Xu and Martin Newcomb*

Department of Chemistry, University of Illinois at Chicago, 845 West Taylor Street, Chicago, Illinois 60607

men@uic.edu

Received June 29, 2005



A model for glycol radicals was employed in laser flash photolysis kinetic studies of catalysis of the fragmentation of a methoxy group adjacent to an α -hydroxy radical center. Photolysis of a phenylselenenylmethylcyclopropane precursor gave a cyclopropylcarbinyl radical that rapidly ring opened to the target α -hydroxy- β -methoxy radical (**3**). Heterolysis of the methoxy group in **3** gave an enyl radical (**4a**) or an enol ether radical cation (**4b**), depending upon pH. Radicals **4** contain a 2,2-diphenylcyclopropane reporter group, and they rapidly opened to give UV-observable diphenylalkyl radicals as the final products. No heterolysis was observed for radical **3** under neutral conditions. In basic aqueous acetonitrile solutions, specific base catalysis of the heterolysis was observed; the pK_a of radical **3** was determined to be 12.5 from kinetic titration plots, and the ketyl radical formed by deprotonation of **3** eliminated methoxide with a rate constant of $5 \times 10^7 \text{ s}^{-1}$. In the presence of carboxylic acids in acetonitrile solutions, radical **3** eliminated methanol in a general acid-catalyzed reaction, and rate constants for protonation of the methoxy group in **3** by several acids were measured. Radical **3** also reacted by fragmentation of methoxide in Lewis-acid-catalyzed heterolysis reactions; ZnBr_2 , $\text{Sc}(\text{OTf})_3$, and BF_3 were found to be efficient catalysts. Catalytic rate constants for the heterolysis reactions were in the range of 3×10^4 to $2 \times 10^6 \text{ s}^{-1}$. The Lewis-acid-catalyzed heterolysis reactions are fast enough for kinetic competence in coenzyme B₁₂ dependent enzyme-catalyzed reactions of glycols, and Lewis-acid-catalyzed cleavages of β -ethers in radicals might be applied in synthetic reactions.

Introduction

Coenzyme B₁₂ dependent diol dehydratase enzymes catalyze the dehydration of glycols to aldehydes via a radical rearrangement reaction (Figure 1).^{1–3} After binding substrate, the cobalt–carbon bond of the coenzyme cleaves to give the 5′-deoxyadenosin-5′-yl radical (Ado•). Ado• abstracts a hydrogen atom from C1 of substrate to give an α,β -dihydroxyalkyl radical (a glycol radical) that rearranges to a β,β -dihydroxy radical. The rearranged radical then abstracts hydrogen atom from the methyl group of 5′-deoxyadenosine to regenerate Ado•, which recombines with cobalt to complete the radical portion of the reaction. The aldehyde hydrate thus formed dehydrates to give the final product.

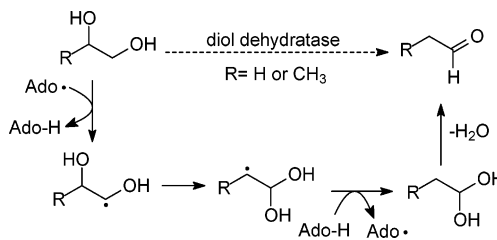


FIGURE 1. Catalytic sequence in coenzyme B₁₂ dependent diol dehydratase catalyzed dehydration of glycols.

Simple glycol radicals are relatively stable kinetically, and the diol dehydratase enzymes catalyze the rearrangement reaction in addition to producing the substrate radical. The mechanism of catalysis is not clear, however, nor is the detailed reaction pathway apparent. The rearrangement reaction might involve a fragmenta-

(1) Toraya, T. In *Chemistry and Biochemistry of B₁₂*; Banerjee, R., Ed.; Wiley: New York, 1999; pp 783–809.

(2) Toraya, T. *Chem. Rev.* **2003**, *103*, 2095–2127.

(3) Toraya, T. *Chem. Rec.* **2002**, *2*, 352–366.

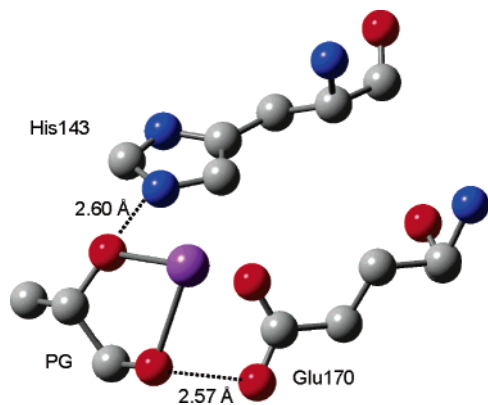


FIGURE 2. Portion of the active site of diol dehydratase from ref 12 (PDB file 1EEX). In the catalytic reaction, the hydroxy group at C2 of propylene glycol migrates to C1.

tion step followed by recombination, or it might occur by a concerted migration pathway. Many experimental results suggest a dissociative pathway as found for acid- or base-catalyzed reactions of glycol radicals in aqueous solutions.^{4–6} Computational results generally favor a concerted migration process,^{7,8} undoubtedly in part because computations of small systems in vacuo do not address charge separation well. The computational barrier for the concerted migration of the hydroxy group is too great for kinetic competence in the enzyme-catalyzed process, but the migration is computed to be catalyzed by acid and/or base.⁹ A recent large QM/MM computational study found low-energy catalytic pathways for both fragmentation/recombination and concerted migration pathways, and the authors favored concerted migration of OH with base catalysis by a glutamate residue in the enzyme.¹⁰

Crystal structures of the diol dehydratase enzyme complexed with substrate do not provide conclusive evidence for the mechanism of the radical reaction.^{11–13} In the active site of resting enzyme with substrate bound (Figure 2), the migrating hydroxy group is hydrogen bonded to a histidine residue, offering the potential for Brønsted acid catalysis, and the nonmigrating hydroxy group is near the carboxylate of a glutamate, permitting the possibility of base catalysis. Perhaps the most interesting feature of the crystal structures is the position of a requisite potassium ion, which is complexed by both oxygens atoms of substrate in the resting enzyme.

(4) Buley, A. L.; Norman, R. O. C.; Pritchett, R. J. *J. Chem. Soc.*, **1966**, 849–852.

(5) Walling, C.; Johnson, R. A. *J. Am. Chem. Soc.* **1975**, *97*, 2405–2407.

(6) Steenken, S. *J. Phys. Chem.* **1979**, *83*, 595–599.

(7) Toraya, T.; Yoshizawa, K.; Eda, M.; Yamabe, T. *J. Biochem.* **1999**, *126*, 650–654.

(8) Eda, M.; Kamachi, T.; Yoshizawa, K.; Toraya, T. *Bull. Chem. Soc. Jpn.* **2002**, *75*, 1469–1481.

(9) Smith, D. M.; Golding, B. T.; Radom, L. *J. Am. Chem. Soc.* **2001**, *123*, 1664–1675.

(10) Kamachi, T.; Toraya, T.; Yoshizawa, K. *J. Am. Chem. Soc.* **2004**, *126*, 16207–16216.

(11) Shibata, N.; Masuda, J.; Tobimatsu, T.; Toraya, T.; Suto, K.; Morimoto, Y.; Yasuoka, N. *Structure* **1999**, *7*, 997–1008.

(12) Masuda, J.; Shibata, N.; Morimoto, Y.; Toraya, T.; Yasuoka, N. *Structure* **2000**, *8*, 775–788.

(13) Yamanishi, M.; Yunoki, M.; Tobimatsu, T.; Sato, H.; Matsui, J.; Dokiya, A.; Iuchi, Y.; Oe, K.; Suto, K.; Shibata, N.; Morimoto, Y.; Yasuoka, N.; Toraya, T. *Eur. J. Biochem.* **2002**, *269*, 4484–4494.

Potassium ion (or other Lewis acids) have long been known to be required for diol dehydratase enzyme activity.^{14,15} Lewis-acid-catalysis of a radical heterolysis such as might occur in diol dehydratase enzymes would be expected, and we recently reported ZnBr₂ catalysis of such reactions.¹⁶ Somewhat surprisingly, computational results suggest that a Lewis acid complexed to the oxygen atoms in a glycol radical would have a minor effect^{7,8,17} or even be anticatalytic for a concerted hydroxy group migration.⁹

In this work, we describe laser flash photolysis studies of reactions of a model for glycol radicals that is subject to acid-, base-, and Lewis-acid-catalyzed heterolytic fragmentation. Each type of catalysis was achieved, but Lewis acid catalysis of the fragmentation satisfies the condition of kinetic competence for the enzyme-catalyzed reaction under mild conditions. The results suggest not only that a Lewis-acid-catalyzed radical heterolysis reaction is possible in nature but also that similar catalysis of radical heterolysis reactions might be exploited in synthesis.

Results and Discussion

Design and Syntheses. We wished to study a single system in which the radical reaction could be catalyzed by a variety of conditions and in various solvents. To study base-catalyzed reactions, we needed to generate an α -hydroxy radical, but that presents a difficulty because typical homolytically labile groups geminal to a hydroxy group will eliminate to give a carbonyl compound. Decarboxylative entries to the desired radical, as from a Barton PTOC ester,¹⁸ were possible in principle, but these types of radical precursors are mixed anhydrides that can hydrolyze in aqueous solutions. Acyl phenylselenides cleave homolytically to give acyl radicals that decarboxylate, and this type of precursor was used for production of an RNA radical by Lenz and Giese,¹⁹ but the rates of decarboxylation reactions are highly sensitive to substitution patterns and can be slow.^{20,21} Golding and co-workers generated an α,β -dihydroxy radical via an intramolecular cascade reaction sequence wherein a carbon-centered radical reacted in a 1,5-H atom abstraction process to give the desired radical.²²

Our approach for production of an α -hydroxy radical also involved a radical cascade sequence to relay a radical center to the hydroxyl-substituted carbon (Scheme 1). We used a fast cyclopropylcarbinyl radical ring-opening reaction as the relay step so that the kinetics of formation of the model radical would not be convoluted with the

(14) Lee, H. A., Jr.; Abeles, R. H. *J. Biol. Chem.* **1963**, *238*, 2367–2373.

(15) Toraya, T.; Sugimoto, Y.; Tamao, Y.; Shimizu, S.; Fukui, S. *Biochemistry* **1971**, *10*, 3475–3484.

(16) Miranda, N.; Xu, L.; Newcomb, M. *Org. Lett.* **2004**, *6*, 4511–4514.

(17) Toraya, T.; Eda, M.; Kamachi, T.; Yoshizawa, K. *J. Biochem.* **2001**, *130*, 865–872.

(18) Barton, D. H. R.; Crich, D.; Motherwell, W. B. *Tetrahedron* **1985**, *41*, 3901–3924.

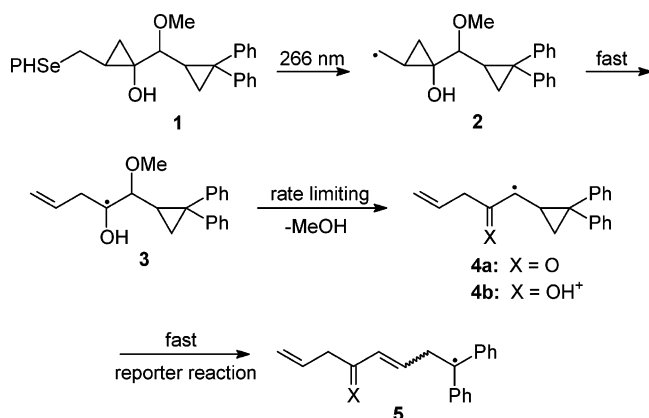
(19) Lenz, R.; Giese, B. *J. Am. Chem. Soc.* **1997**, *119*, 2784–2794.

(20) Beckwith, A. L. J.; Crich, D.; Duggan, P. J.; Yao, Q. W. *Chem. Rev.* **1997**, *97*, 3273–3312.

(21) Chatgililoglu, H.; Crich, D.; Komatsu, M.; Ryu, I. *Chem. Rev.* **1999**, *99*, 1991–2069.

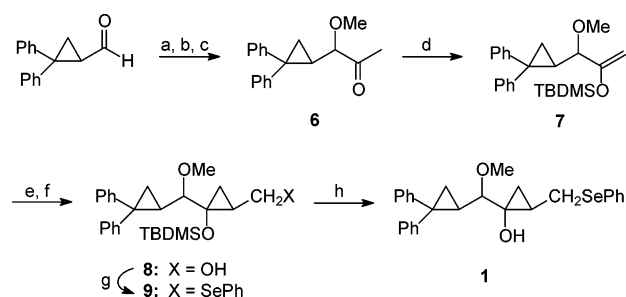
(22) Anderson, R. J.; Ashwell, S.; Garnett, I.; Golding, B. T. *J. Chem. Soc., Perkin Trans. 1* **2000**, 4488–4498.

SCHEME 1



kinetics of the fragmentation reaction that was the object of the study. A phenylselenenyl group provided the photo-sensitive moiety; alkyl phenyl selenides are stable in aqueous solutions but are cleaved with reasonable efficiency by 266-nm light.²³ Photolysis of precursor **1** gave the cyclopropylcarbinyl radical **2**. Ring opening of radical **2** to give α -hydroxy radical **3** was expected to be highly regioselective and to occur at ambient temperature with a rate constant in the range of $5\text{--}10 \times 10^9 \text{ s}^{-1}$ by analogy to the rate constants for ring opening of alkoxy-substituted cyclopropylcarbinyl radicals.^{24,25} Fragmentation of the methoxy group in **3** under basic or acidic conditions would give, respectively, an enyl radical (**4a**) or an enol radical cation (**4b**). The initial product radicals **4** contain a reporter group for UV detection;²⁶ rapid ring opening of radicals **4** to detectable radicals **5** was expected based on the fast rearrangement of the parent radical, (2,2-diphenylcyclopropyl)methyl, which ring opens with a rate constant of $5 \times 10^{11} \text{ s}^{-1}$ at ambient temperature.²⁷

The hydroxy group in radical **3** provides a model for a glycol radical that can react with base catalysis, but at the expense of some mechanistic ambiguity. If methoxy group migration in **3** were to occur instead of heterolysis, the product formed would be a β -hydroxy- β -methoxy radical (**4**, X = OH, OMe), and this radical would “report” in the same manner as other radicals **4**. One cannot distinguish between heterolysis and migration reactions by trapping the final products in preparative reactions because the ultimate product from migration would be a hemiacetal that eliminates methanol. Nonetheless, methoxy group heterolysis instead of migration was expected by analogy to numerous fragmentation reactions of glycol radicals.^{4,5} In addition, a closely related α -methoxy- β -methoxy radical containing the same reporter group gave no acetal product when it reacted in acid-catalyzed and zinc(II)-catalyzed reactions.^{16,28}

SCHEME 2^a

^a Key: (a) lithium acetylide, 10–22 °C; (b) HgO, 5% H₂SO₄, 60 °C; (c) (CH₃)₃OBF₄, proton-sponge; (d) LDA, *tert*-butyldimethylsilyl chloride (TBDMS-Cl), –78 °C; (e) EtO₂CCHN₂, Cu(acac)₂, benzene, reflux; (f) LiAlH₄, ambient; (g) *N*-phenylselenylphthalimide, Bu₃P, 0 °C; (h) DIBAL-H, 0 to 22 °C.

The synthetic sequence to radical precursor **1** is shown in Scheme 2. Addition of lithium acetylide to the aldehyde followed by mercuric oxide catalyzed hydrolysis of the alkyne and methylation of the hydroxy group gave ketone **6**. One diastereomer of **6** was carried forward in the synthesis. Enolization of **6** and treatment with *tert*-butyldimethylsilyl chloride gave the silyl enol ether **7**. Cyclopropanation of **7** with ethyl diazoacetate followed by LiAlH₄ reduction of the ester group gave intermediate **8**. One diastereomer of **8** was carried forward in the synthesis by conversion of the alcohol group to the phenylselenenyl group (**9**). Removal of the silyl group in **9** gave radical precursor **1**.

Most of the reactions in the synthetic sequence proceeded smoothly, but the silyl protecting group presented difficulties. In an attempt to use the trimethylsilyl group for protection (i.e., intermediate **7** but with the trimethylsilyl group in place of TBDMS), the yields in the cyclopropanation reaction and in the ester reduction reaction were poor. The TBDMS group worked well for protection in these two reactions, but its removal at the end of the synthesis was problematic; attempted removal of this group with fluoride under a variety of conditions resulted in fragmentation of the cyclopropyl ring. Eventually, we were able to remove the TBDMS group with DIBAL-H by the method of Corey and Jones,²⁹ which gave precursor **1** in an acceptable yield.

Radical precursor **1** contains four stereogenic carbons, but two of these stereogenic centers are lost in the production of radical **3**. Therefore, we did not attempt to assign the complete relative stereochemistry in precursor **1**, although this compound was isolated as a single diastereomer. The stereogenic centers that remain in radical **3** are those present in the intermediate ketone **6**. For the two diastereomers of **6**, the coupling constants between the proton on the methoxy-substituted carbon and the adjacent cyclopropyl proton were 10.2 Hz (isomer **6a**), which was carried forward in the synthesis of **1** and 8.1 Hz (isomer **6b**). We used a modeling program to estimate the relative energies of the conformations of **6** and to calculate the weighted average coupling constants. This exercise indicated that the syn diastereomer should have a coupling constant of ca. 4 Hz, and the anti diastereomer should have a coupling constant of ca. 11 Hz. From this result and the large coupling constant in

(23) Miranda, N.; Daublain, P.; Horner, J. H.; Newcomb, M. *J. Am. Chem. Soc.* **2003**, *125*, 5260–5261.

(24) Le Tadic-Biadatti, M. H.; Newcomb, M. *J. Chem. Soc., Perkin Trans. 2* **1996**, 1467–1473.

(25) Martinez, F. N.; Schlegel, H. B.; Newcomb, M. *J. Org. Chem.* **1998**, *63*, 3618–3623.

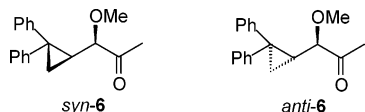
(26) Newcomb, M.; Tanaka, N.; Bouvier, A.; Tronche, C.; Horner, J. H.; Musa, O. M.; Martinez, F. N. *J. Am. Chem. Soc.* **1996**, *118*, 8505–8506.

(27) Newcomb, M.; Johnson, C. C.; Manek, M. B.; Varick, T. R. *J. Am. Chem. Soc.* **1992**, *114*, 10915–10921.

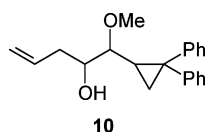
(28) Newcomb, M.; Miranda, N. *J. Org. Chem.* **2004**, *69*, 6515–6520.

(29) Corey, E. J.; Jones, G. B. *J. Org. Chem.* **1992**, *57*, 1028–1029.

isomer **6a**, we tentatively assign the structure of isomer **6a** as the anti diastereomer.



The experimental design in Scheme 1 indicates fast and regioselective rearrangement of radical **2** to give target radical **3**, which was expected to be relatively stable. Preparative reactions of precursor **1** in the presence of Bu_3SnH in THF and in CH_3CN solutions confirmed the desired properties in a qualitative sense. In a reaction conducted at ambient temperature in the presence of ca. 0.006 M Bu_3SnH in CH_3CN , we obtained products **10**, from trapping of radical **3**, as a mixture of diastereomers in a ca. 55:45 ratio as determined from the NMR spectrum of the crude reaction product. Note that the tin hydride trapping reaction of radical **3** creates a new stereogenic atom. Silica gel chromatography resulted in isolation of the mixture of diastereomers and enrichment of one such that the ratio was ca. 80:20. In a reaction with 0.1 M Bu_3SnH in THF, the same diastereomers (in a 60:40 ratio) were found as determined by NMR spectroscopy of the crude reaction mixtures, and the yield of these products was estimated to be >70% from evaluation of the NMR spectrum of the crude reaction mixture. Thus, in a qualitative comparison to trapping by tin hydride, ring opening of radical **2** to radical **3** is fast, and fragmentation of radical **3** to give, ultimately, radical **5** is slow. The ring opening of radical **2** was expected to be on the order of 10^9 to 10^{10} s^{-1} ,^{24,25} which is much faster than trapping a primary alkyl radical with Bu_3SnH ($k = 2 \times 10^6 \text{ M}^{-1} \text{ s}^{-1}$ at ambient temperature).^{30,31} Reactions of Bu_3SnH with α -methoxy radicals have second-order rate constant of $3\text{--}4 \times 10^5 \text{ M}^{-1} \text{ s}^{-1}$ at ambient temperature,^{32,33} and the preparative results suggest that the heterolytic cleavage of radical **3** has a rate constant at ambient temperature of $k < 3000 \text{ s}^{-1}$.



Laser Flash Photolysis Studies. When radical **3** was produced in laser flash photolysis studies in a variety of solvents, no growth in signal was observed in the region of the UV–visible spectrum where product **5** was expected to absorb. When various catalysts were present, however, strong signals grew in at the expected wavelengths. Figure 3 shows a typical set of results from reaction of **3**. This figure shows a time-resolved spectrum from reaction of **3** in a basic aqueous acetonitrile solution. The product from reaction of **3** is growing in with $\lambda_{\text{max}} \approx$

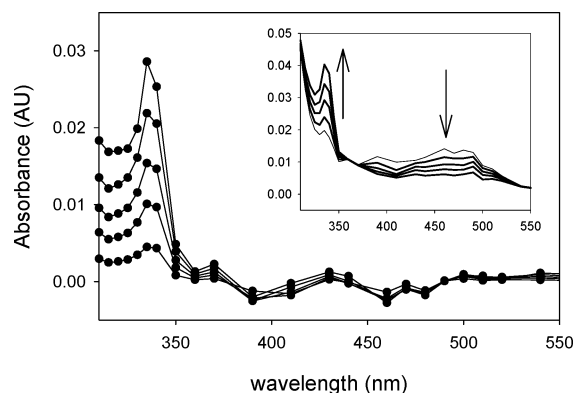


FIGURE 3. Typical time-resolved growth spectrum for formation of radical **5**; the signal is growing in over ca. 6 μs . A background spectrum of the decaying phenylselenyl radical was subtracted at each time slice, and an early time spectrum was subtracted to give a baseline. The inset shows the same data set without subtracting the spectrum of the phenylselenyl radical.

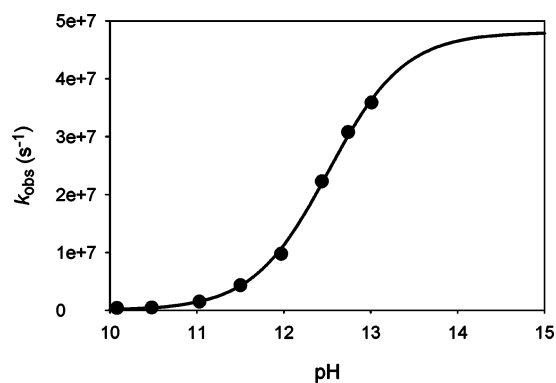


FIGURE 4. Observed rate constants for reactions of radical **3** in aqueous acetonitrile solutions. The line shows the calculated observed rate constants for $\text{p}K_{\text{a}} = 12.51$ and $k_{\text{B}} = 4.8 \times 10^7 \text{ s}^{-1}$ (see text).

335 nm. The byproduct of the photolysis reaction is the phenylselenyl radical, which displays an absorbance at ca. 290 nm and another broad absorbance from 370 to 530 nm. The signal from the PhSe radical is decaying in the inset in Figure 3. A time-resolved spectrum of decay of the PhSe radical, produced by photolysis of a simple alkyl phenyl selenide under otherwise similar conditions, was subtracted from the corresponding time slices to give the time-resolved spectrum in Figure 3 that is due mainly to the ultimate diphenylalkyl radical product **5** ($\text{X} = \text{O}$).

Base-Catalyzed Heterolysis Reaction. Reactions of radical **3** under basic conditions were studied in water–acetonitrile (1:1, v:v) mixtures. Figure 4 shows the kinetic results. In this figure, the pH values below 12 are the measured pH values for aqueous solutions of buffers before mixing with acetonitrile, and the pH values for 12 and greater are the calculated pH values for aqueous solutions based on the concentration of NaOH. The pH values in the cosolvent mixture will shift, but this shift will be paralleled by a shift in the $\text{p}K_{\text{a}}$ of radical **3**;³⁴

(30) Chatgililoglu, C.; Ingold, K. U.; Scaiano, J. C. *J. Am. Chem. Soc.* **1981**, *103*, 7739–7742.

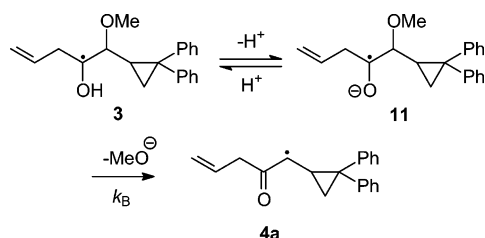
(31) Chatgililoglu, C.; Newcomb, M. *Adv. Organomet. Chem.* **1999**, *44*, 67–112.

(32) Beckwith, A. L. J.; Glover, S. A. *Aust. J. Chem.* **1987**, *40*, 157–173.

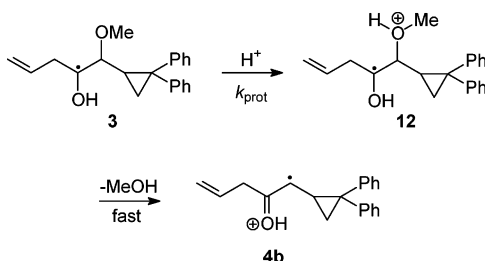
(33) Johnson, C. C.; Horner, J. H.; Tronche, C.; Newcomb, M. *J. Am. Chem. Soc.* **1995**, *117*, 1684–1687.

(34) Espinosa, S.; Bosch, E.; Roses, M. *Anal. Chem.* **2000**, *72*, 5193–5200.

SCHEME 3



SCHEME 4



therefore, we employed the aqueous pH values in the data analysis and plot to provide a direct measure of the pK_a of radical **3** in water.

The pH dependence of the rate constants for reaction of radical **3** in Figure 4 describes a typical kinetic titration curve indicating that the reaction is specific base catalyzed (Scheme 3). Equilibration between radical **3** and its anionic form (ketyl **11**) is fast, and fragmentation of the methoxide group is the rate-limiting step. The kinetic data was solved according to eq 1, where k_{obs} is the observed rate constant, K_a is the acidity constant for radical **3**, and k_B is the rate constant for fragmentation of radical **11**. The best fit gave a pK_a for radical **3** of 12.51 ± 0.05 and a first-order rate constant for elimination of methoxide ion from ketyl **11** of $k_B = (4.8 \pm 0.3) \times 10^7 \text{ s}^{-1}$ (errors at 2σ). The pK_a for radical **3** is similar to those of simple α -hydroxyalkyl radicals.^{35,36} The rate constant for loss of methoxide from ketyl **11** is about 1 order of magnitude larger than the rate constant for loss of hydroxide from glycol radical anions;⁶ this value indicates a balance between a retarding effect of the methoxide group elimination in comparison to an hydroxide group and an accelerating effect of the cyclopropane reporter group.²⁸

$$k_{obs} = (k_B \times 10^{(pH)} \times K_a) / (K_a \times 10^{(pH)} + 1) \quad (1)$$

Acid-Catalyzed Reactions of Radical 3. In acetonitrile solutions with added carboxylic acids, acid-catalyzed heterolysis reactions could be quantified. The observed rate constants increased linearly with acid concentration (Supporting Information), indicating a general acid-catalyzed reaction with rate-limiting protonation of **3** and fast elimination of neutral methanol from radical cation **12** (Scheme 4). This mechanism is the same as that for dehydration of glycol radicals in water, where rate-limiting protonation was found.³⁷ Second-order rate

(35) Laroff, G. P.; Fessenden, R. W. *J. Phys. Chem.* **1973**, *77*, 1283–1288.

(36) Akhlaq, M. S.; Murthy, C. P.; Steenken, S.; von Sonntag, C. *J. Phys. Chem.* **1989**, *93*, 4331–4334.

(37) Steenken, S.; Davies, M. J.; Gilbert, B. C. *J. Chem. Soc., Perkin Trans. 2* **1986**, 1003–1010.

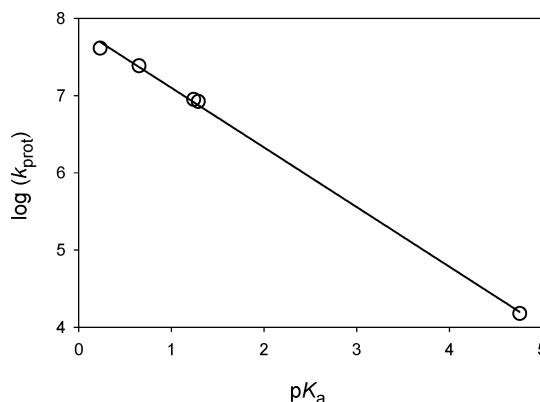
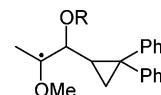


FIGURE 5. Logarithm of second-order rate constants for protonation of radical **3** in acetonitrile by carboxylic acids (k_{prot}) against the aqueous pK_a values of the acids; the slope is -0.77 .

constants for protonation (k_{prot}) were obtained from eq 2, where k_{obs} is the observed rate constant, k_0 is the background rate constant, and [acid] is the concentration of acid. For a series of carboxylic acids, the protonation rate constants correlated well with the aqueous pK_a values of the acids (Figure 5).

$$k_{obs} = k_0 + k_{prot}[\text{acid}] \quad (2)$$

The acid-catalyzed reactions of radical **3** in acetonitrile are similar to those of the related α,β -dimethoxy radical **13a**.²⁸ In both cases, protonation of the β -methoxy group gives a distonic radical cation that can react in a heterolytic fragmentation step with loss of a neutral methanol molecule to give a conjugated radical cation. General acid catalysis was demonstrated for cleavage in radical **13a**, and the rate constants for protonation of **13a** in acetonitrile were similar to those for protonation of **3**.²⁸ The fast fragmentation of neutral methanol from protonated radical cation **12**, as well as from the radical cation formed by protonation of **13a**,²⁸ is consistent with the observation that loss of the anionic phosphate group in radical **13b** occurs with a rate constant exceeding $1 \times 10^8 \text{ s}^{-1}$.²⁸ In aqueous solutions, elimination of neutral water from protonated glycol radical cations is faster than the protonation reaction.³⁷



13a: R = Me
13b: R = P(O)(OEt)₂

Lewis-Acid-Catalyzed Reactions of 3. Lewis-acid-catalyzed heterolytic fragmentations of radical **3** are the most interesting reactions we studied because there exists little data for such reactions. Zinc bromide catalysis of the fragmentation reaction of **3** in acetonitrile was noted previously in a preliminary report,¹⁶ and we have now also studied catalysis by Sc(OTf)₃ and BF₃. Radical precursor **1** was stable in acetonitrile or THF solutions containing these Lewis acids, and reactions were conducted by photochemical production of radical **3** in the presence of varying concentrations of the Lewis acids.

Figure 6 shows the results for reactions of **3** in the presence of Sc(OTf)₃ in THF solutions. We found variable

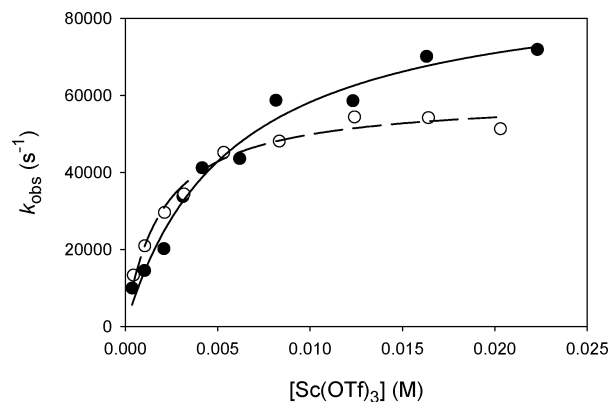
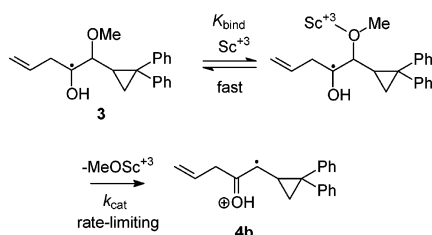


FIGURE 6. Observed rate constants for reactions of radical **3** in the presence of $\text{Sc}(\text{OTf})_3$ in THF solutions containing 0.05 M water (grey, dashed line) and 0.10 M water (black, solid line). The lines are regression fits discussed in the text.

SCHEME 5



results when the reactions were conducted in “anhydrous” THF, which apparently was related to irreproducible small concentrations of water in the solutions. When water was added to the THF solutions to give 0.05 and 0.10 M aqueous mixtures, the kinetic results were reproducible. The observed rate constants increased with increasing concentration of the scandium salt to reach or approach a limiting plateau value.

The kinetic behavior found with $\text{Sc}(\text{OTf})_3$ in aqueous THF solutions is a clear indication of saturation kinetics (Scheme 5). A reactive complex is formed reversibly, and fragmentation of the complex is the rate-limiting step. Similar behavior was previously found for reactions of radical **3** in the presence of ZnBr_2 in acetonitrile solutions.¹⁶ The kinetic results were treated according to eq 3 where k_{obs} is the observed rate constant, $[\text{LA}]$ is the molar concentration of Lewis acid, K_{bind} is the binding constant for formation of the complex, and k_{cat} is the catalytic rate constant for reaction of the complex.

$$k_{\text{obs}} = (k_{\text{cat}}K_{\text{bind}}[\text{LA}])/(K_{\text{bind}}[\text{LA}] + 1) \quad (3)$$

The results for ZnBr_2 -catalyzed fragmentation of **3** in acetonitrile¹⁶ and for $\text{Sc}(\text{OTf})_3$ -catalyzed fragmentation of **3** in THF are listed in Table 1. Note that a change in the amount of water in the THF solutions affected both the binding constant of the salt and the catalytic rate constant for reaction of the complex. As the water concentration was increased, the binding constant was reduced as one might expect and the catalytic rate constant increased. Further studies are necessary to identify the origin of the kinetic effect, which might be due to specific changes in solvation of the cation, to general base catalysis by water, or to a change in polarity of the solvent. A change in rate constants due to a solvent

TABLE 1. Binding Constants and Rate Constants for Lewis Acid Catalyzed Reactions of Radical **3**

salt	solvent	K_{bind} (M^{-1})	k_{cat} (s^{-1})
ZnBr_2^a	CH_3CN	1000	2.8×10^4
$\text{Sc}(\text{OTf})_3$	0.05 M H_2O in THF	510 ± 60	$(6.0 \pm 0.2) \times 10^4$
	0.10 M H_2O in THF	180 ± 30	$(9.1 \pm 0.6) \times 10^4$
$\text{BF}_3(\text{OEt}_2)$	CH_3CN	$(9.0 \pm 0.5) \times 10^5$	$(1.52 \pm 0.01) \times 10^6$
	CH_3CN	6.25×10^{10b}	$(1.56 \pm 0.02) \times 10^6$

^a Reference 16. ^b Binding constant in units of $(\text{M}^{-1})^2$ for formation of a complex with $(\text{BF}_3)_2$.

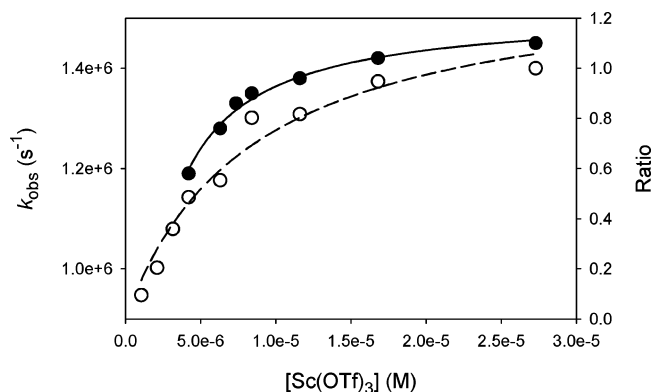


FIGURE 7. Effect of $\text{Sc}(\text{OTf})_3$ on reactions of radicals **2** and **3** in acetonitrile. The solid symbols are observed rate constants (left scale) for reactions of radical **3**. The open symbols show the ratios (right scale) of “instant” signal at a given concentration of salt relative to that observed with 2.7×10^{-5} M salt. The lines are regression fits for saturation behavior.

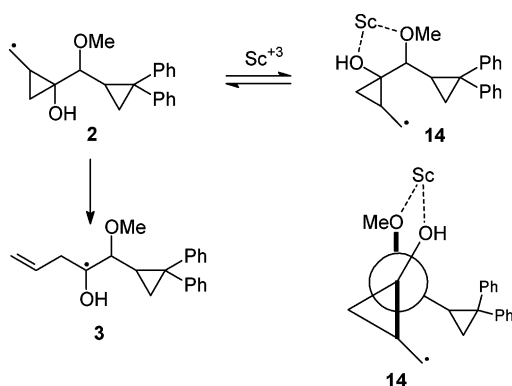
polarity effect (i.e., an environment effect) appeared to be supported by the kinetic results obtained in acetonitrile discussed below.

Studies of $\text{Sc}(\text{OTf})_3$ catalysis of the reactions of radical **3** in acetonitrile were complex. A concentration-dependent increase in the rate of reaction of radical **3** was observed as above, but a new phenomenon was also observed. As the concentration of $\text{Sc}(\text{OTf})_3$ was increased, the amount of instantaneous absorbance at 335 nm increased. This behavior is shown in Figure 7, where the open symbols show the ratio of instantaneous growth relative to the amount observed at high salt concentration. This new effect appears to result from an interaction of $\text{Sc}(\text{OTf})_3$ with radical **2** (see below).

The “slow” signal growth in the presence of $\text{Sc}(\text{OTf})_3$ in acetonitrile was analyzed in a manner similar to that used for the Lewis acid kinetic effects in THF discussed above. The rate of signal growth increased as a function of salt concentration. Solution of these data via eq 3 gave a binding constant and catalytic rate constant for $\text{Sc}(\text{OTf})_3$ in CH_3CN that is included in Table 1. Both the binding constant and catalytic rate constant were greatly increased in acetonitrile in comparison to the values found in THF solutions. Increases in both values were expected because salt binding energies of CH_3CN should be reduced from those of aqueous THF, resulting in a larger K_{bind} value for radical **3**, and the catalytic rate constant for the charge-forming heterolysis reaction should increase for CH_3CN , which is considerably more polar than THF as judged by $E_{\text{T}}(30)$ values.³⁸ Radical heterolysis rate constants for loss of anionic leaving

(38) Reichardt, C. *Chem. Rev.* **1994**, *94*, 2319–2358.

SCHEME 6



groups were previously found to correlate well with solvent polarity values.^{39–46}

The fast signal growth found in $\text{Sc}(\text{OTf})_3$ -catalyzed reactions in CH_3CN appears to result from a new reaction channel that gives product **5** directly from radical **2** without the intermediacy of uncomplexed radical **3**. The amount of instantaneous signal growth can be analyzed as a function of concentration of $\text{Sc}(\text{OTf})_3$ in a manner similar to that used to analyze the rate constants for the slow reaction. Thus, the ratio of “instant” signal at low salt concentration relative to the amount at high salt concentration as a function of $\text{Sc}(\text{OTf})_3$ concentration is shown in Figure 7. The data were analyzed by eq 4, where *Ratio* is the amount of instant signal growth compared to a measured value at high salt concentration, *F* is the fraction of total fast signal growth at the reference value relative to the total computed from the regression analysis ($0 < F < 1$), K_{bind} is a binding constant for the Lewis acid complexation with radical **2**, and $[\text{LA}]$ is the molar concentration of Lewis acid. For reactions in CH_3CN , we obtained $F = 0.72$ and $K_{\text{bind}} = (1.2 \pm 0.2) \times 10^5 \text{ M}^{-1}$.

$$\text{Ratio} = ((1/F)K_{\text{bind}}[\text{LA}] / (K_{\text{bind}}[\text{LA}] + 1)) \quad (4)$$

The effect that leads to the “instant” conversion of radical **2** to radical **5** is not obvious, but it appears to be related directly to the Lewis acidity strength of the salt and inversely to the basicity of the solvent. Thus, the effect was only noticeable for the strong Lewis acid $\text{Sc}(\text{OTf})_3$ in the relatively low basicity solvent CH_3CN . We speculate that Lewis acid complexation of radical **2** before the ring opening that gives radical **3** might lead to a highly reactive conformation (e.g., radical **14**) that can

(39) Choi, S. Y.; Crich, D.; Horner, J. H.; Huang, X. H.; Martinez, F. N.; Newcomb, M.; Wink, D. J.; Yao, Q. *J. Am. Chem. Soc.* **1998**, *120*, 211–212.

(40) Choi, S. Y.; Crich, D.; Horner, J. H.; Huang, X. H.; Newcomb, M.; Whitted, P. O. *Tetrahedron* **1999**, *55*, 3317–3326.

(41) Whitted, P. O.; Horner, J. H.; Newcomb, M.; Huang, X. H.; Crich, D. *Org. Lett.* **1999**, *1*, 153–156.

(42) Newcomb, M.; Horner, J. H.; Whitted, P. O.; Crich, D.; Huang, X. H.; Yao, Q. W.; Zipse, H. *J. Am. Chem. Soc.* **1999**, *121*, 10685–10694.

(43) Newcomb, M.; Miranda, N.; Huang, X. H.; Crich, D. *J. Am. Chem. Soc.* **2000**, *122*, 6128–6129.

(44) Bales, B. C.; Horner, J. H.; Huang, X. H.; Newcomb, M.; Crich, D.; Greenberg, M. M. *J. Am. Chem. Soc.* **2001**, *123*, 3623–3629.

(45) Bagnol, L.; Horner, J. H.; Newcomb, M. *Org. Lett.* **2003**, *5*, 5055–5058.

(46) Horner, J. H.; Bagnol, L.; Newcomb, M. *J. Am. Chem. Soc.* **2004**, *126*, 14979–14987.

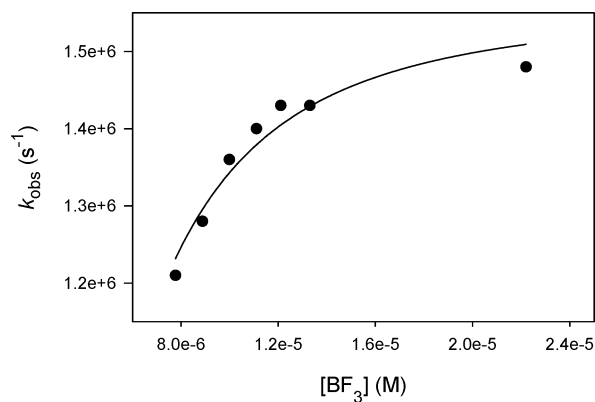


FIGURE 8. Observed rate constants for reactions of radical **3** in acetonitrile in the presence of BF_3 etherate. The line is the regression fit of the data against the square of BF_3 concentration according to eq 5.

lose methoxide rapidly without passing through noncomplexed radical **3**. For example, simultaneous cleavage of the two bold bonds shown in the Newman projection of **14** might bypass radical **3** (Scheme 6). Further studies of the origin of this unusually fast $\text{Sc}(\text{OTf})_3$ -dependent reaction should be interesting because structural effects on the kinetics of radical fragmentation reactions might be important in the diol dehydratase-catalyzed reaction.

Catalysis of the heterolysis reaction of radical **3** with BF_3 in CH_3CN also was apparent. Saturation kinetic behavior was observed (Figure 8), but the data was not fit well for the model of binding by monomeric BF_3 . When the data was solved for the square of BF_3 concentration via eq 5, however, a good fit was obtained, indicating that dimeric BF_3 was the active catalyst. The rate constant for reaction of the $(\text{BF}_3)_2$ -complexed radical was similar to that for the $\text{Sc}(\text{OTf})_3$ -complexed radical (Table 1). In this case, however, K_{bind} is a complex term that includes the dimerization equilibrium constant for BF_3 .

$$k_{\text{obs}} = (k_{\text{cat}}K_{\text{bind}}[\text{LA}]^2) / (K_{\text{bind}}[\text{LA}]^2 + 1) \quad (5)$$

It is interesting to note that the rate constants for heterolysis of **3**– $\text{Sc}(\text{OTf})_3$ and **3**– $(\text{BF}_3)_2$ complexes in acetonitrile were the same. In terms of stabilization of the charge on the departing methoxy groups, these two Lewis acids are comparable, and both are better in this regard than ZnBr_2 . In terms of efficiency, $\text{Sc}(\text{OTf})_3$ is superior to BF_3 in acetonitrile because it forms a more stable complex with the radical, a likely result of bidentate binding of the scandium ion by the vicinal methoxy and hydroxy groups in **3**.

Implications for Diol Dehydratase Catalyzed Reactions. The uncertainty about the method of catalysis of the diol dehydratase enzyme results in part from the fact that X-ray crystal structures reveal that any type of catalysis might be rationalized as shown in Figure 2. Thus, imidazole from His143 is close to the migrating β -hydroxy group of substrate, suggesting the possibility of acid catalysis; carboxylate from Glu170 is close to the α -hydroxy group of substrate, suggesting the possibility of base catalysis, and potassium ion is bound by both hydroxy groups of substrate. Computational studies favor concerted migrations of the β -hydroxy group, with one

group emphasizing a potential acid-catalyzed reaction,^{9,47} and one concluding that base catalysis is more important.¹⁰ The latter conclusion is consistent with the experimental observation that the enzyme is functional in basic but not acidic solutions.^{14,15}

In regard to base-catalyzed reactions, concerted migrations of hydroxy groups in glycol radicals have not been demonstrated experimentally. Base-catalyzed heterolytic fragmentations of glycol radicals give stable enolyl radicals,⁶ and we found specific base catalysis in the heterolytic fragmentation of radical **3**, similar to the results with glycol radicals. The rate constant for methoxide fragmentation in ketyl **11**, $k = 5 \times 10^7 \text{ s}^{-1}$, is about 1 order of magnitude larger than those found for fragmentation of hydroxide from α -hydroxy ketyl radicals⁶ due to the accelerating effect of the cyclopropyl reporter group²⁸ but not fast enough to observe general base catalysis. Ribonucleotide reductase catalyzes the elimination of water from ribonucleotide radicals, a reaction similar to that we studied here, and the water fragmentation reaction in a model was found to be general base catalyzed,¹⁹ but the radical products in the RNR-catalyzed reactions are more stable than enolyl radical **4a** formed from ketyl **11**.

We believe the Lewis acid catalysis of the heterolysis reaction of radical **3** is quite interesting in regard to the mechanism for rearrangement of glycol radicals in the diol dehydratase enzyme. Crystal structures of the resting enzyme with bound substrate show that the glycol substrate is complexed with potassium ion,^{11–13} but the effect of the Lewis acid on heterolytic fragmentation of hydroxide has not been addressed computationally nor previously studied experimentally.

The important values in this work in regard to Lewis acid catalysis in the diol dehydratase enzyme are the catalytic rate constants. Binding constants, while important for bimolecular processes, are not an issue for the enzyme because the potassium ion is held adjacent to substrate. The reporter group in radical **3** accelerates the heterolysis reaction by about a factor of 40,^{28,46} but the methoxy group in **3** is expected to retard the heterolysis reaction in comparison to the heterolysis of a hydroxy group in a glycol radical. On balance, one might expect the catalytic rate constants for hydroxy group fragmentation in a glycol radical to be about 1 order of magnitude smaller than the rate constants we found here. If that is the case, even the poorer catalyst we studied, ZnBr₂, provides adequate kinetic competence for the rearrangement reaction in nature, where the enzyme has an experimental $k_{\text{cat}} = 330 \text{ s}^{-1}$.³ It seems likely that any Lewis acid would provide adequate stabilization for kinetic competence in the enzyme-catalyzed reaction.

Another interesting observation in regard to the enzyme-catalyzed reaction is the considerable environment effect we observed in the Sc(OTf)₃-catalyzed reactions. If the results with aqueous THF solutions are extrapolated to anhydrous THF, then the heterolysis rate constant would be on the order of $k_{\text{cat}} = 1 \times 10^4 \text{ s}^{-1}$, and in the modestly polar solvent acetonitrile, the fragmentation reaction was about 2 orders of magnitude faster than

in relatively low polarity THF. With such a large kinetic effect associated with the modest polarity change, it would appear that diol dehydratase enzymes could employ environment effects to modulate the rates of the fragmentation reactions.

Conclusion

We have described a versatile model for studying heterolysis reactions of a glycol radical model under a variety of catalytic conditions. The alkylphenylselenide precursor **1** is reasonably stable in aqueous solutions and in the presence of acid or base, but it is cleaved relatively efficiently by 266-nm light to give radical **2**. Ring opening of radical **2** rapidly produces the α -hydroxy- β -methoxy radical **3**, and heterolysis of the methoxy group in radical **3** was catalyzed by acids, bases, and Lewis acids. The reporter group in radical **3** provides a strong chromophore in the final radical products, which permits precise kinetic measurements.

Few examples of Lewis-acid-catalyzed radical reactions have been reported previously. Given the generally mild conditions of many Lewis acids and their compatibility with organic solvents, such catalysis might be useful in preparative organic radical chemistry and could be involved in the glycol radical rearrangements in nature.

Experimental Section

Synthetic details for the preparation of precursor **1** are in Supporting Information.

Laser Flash Photolysis Studies were performed with the first diastereomer of **1**. Acetonitrile and THF (high-performance liquid chromatography grade) were used as received. The laser flash photolysis experimental methods were similar to those previously reported.^{23,46} Kinetic spectrometers used Nd:YAG lasers irradiating at 266 nm. Solutions of precursor **1** with an absorbance at 266 nm of 0.4–0.5 AU and containing the appropriate additives were placed in a thermally jacketed addition funnel and degassed by sparging with helium. The solutions were allowed to flow through a flow cell for the laser flash photolysis studies such that fresh solution was used for each experiment. All studies were performed at 20 ± 2 °C.

pH-Dependent Kinetic Studies. Solutions of precursor **1** were prepared in acetonitrile such that the absorbance was 0.8–1.0 AU at 266 nm. Basic buffers and sodium hydroxide solutions were prepared separately. The CH₃CN solution and the basic solution were placed in gastight syringes, and the mixtures were pumped via a syringe pump into a tee that led to the laser flow cell. The pH values of the aqueous buffer solutions were measured before mixing, and these values are the ones given in Figure 4 and in the Supporting Information. The concentration of the sodium hydroxide in strongly basic solutions was determined by titration, and the pH was calculated. The pK_a values of both the buffer acids and α -hydroxy radical **3** will be different in solvent mixtures from the values obtained in water.³⁴ We assumed that the pK_a of the α -hydroxy group in radical **3** will change by the same amount as the pK_a values of the buffer acids. Detailed results are in Supporting Information.

Acknowledgment. This work was supported by a grant from the National Science Foundation (CHE-0235293).

Supporting Information Available: Synthetic methods, detailed kinetic results, NMR spectra. This material is available free of charge via the Internet at <http://pubs.acs.org>.

JO051349D

(47) Smith, D. M.; Golding, B. T.; Radom, L. *J. Am. Chem. Soc.* **1999**, *121*, 5700–5704.